Supplementary Information

Shuvojit Paul, Randhir Kumar, and Ayan Banerjee*
Dept of Physical Sciences, Indian Institute of Science Education and Research, Mohanpur, Kolkata, India 741246 and
**ayan@iiserkol.ac.in*

I. THEORY

Here we outline the major steps in deriving the correlation functions and the complex shear modulus on the Smoluchowski time scale, i.e. the over-damped regime, starting from Langevin equations

$$m_i \dot{\boldsymbol{v}}_i = -\boldsymbol{\gamma}_{ij}\boldsymbol{v}_j - \boldsymbol{\nabla}_i U + \boldsymbol{\xi}_i \tag{1}$$

$$\dot{\mathbf{R}}_i = \boldsymbol{v}_i \tag{2}$$

presented and explained in the main text. Due to the experimental limitation on the data sampling frequency, we can assume the momentum to be rapidly relaxing on the time scale of the trap motion. Therefore, we can adiabatically eliminate the momentum [1, 2] and get,

$$\boldsymbol{\gamma}_{ij}(\mathbf{R}_i^0, \mathbf{R}_j^0)\dot{\mathbf{R}}_j + \boldsymbol{\nabla}_i U = \boldsymbol{\xi}_i \tag{3}$$

$$\langle \boldsymbol{\xi}_i(t)\rangle = \mathbf{0}$$
$$\langle \boldsymbol{\xi}_i(t)\boldsymbol{\xi}_j(t')\rangle = 2k_BT\boldsymbol{\gamma}_{ij}(\mathbf{R}_i^0, \mathbf{R}_j^0)\delta(t-t')$$

Since the trap-center separation is far greater than the standard deviation of the position fluctuations of individual particles, $\boldsymbol{\gamma}_{ij}$ can be considered time-independent and a function of the trap-center separation. Equation (3) can be inverted and presented in terms of approximate mobility tensors $\boldsymbol{\mu}_{ij}(\mathbf{R}_i^0, \mathbf{R}_j^0) = \boldsymbol{\gamma}_{ij}^{-1}(\mathbf{R}_i^0, \mathbf{R}_j^0)$ in the following manner:

$$\dot{\mathbf{R}}_i + \boldsymbol{\mu}_{ij}\boldsymbol{\nabla}_j U = \boldsymbol{\mu}_{ij}\boldsymbol{\xi}_j \tag{4}$$

$$\frac{d}{dt}\begin{bmatrix}\mathbf{R}_1\\ \mathbf{R}_2\end{bmatrix} = -\begin{bmatrix}\mu k_1\boldsymbol{\delta} & \boldsymbol{\mu}_{12}k_2\\ \boldsymbol{\mu}_{21}k_1 & \mu k_2\boldsymbol{\delta}\end{bmatrix}\begin{bmatrix}\mathbf{R}_1\\ \mathbf{R}_2\end{bmatrix} + \begin{bmatrix}\mu\boldsymbol{\delta} & \boldsymbol{\mu}_{12}\\ \boldsymbol{\mu}_{21} & \mu\boldsymbol{\delta}\end{bmatrix}\begin{bmatrix}\boldsymbol{\xi}_1\\ \boldsymbol{\xi}_2\end{bmatrix}$$

where $\boldsymbol{\mu}_{11} = \mu\boldsymbol{\delta} = \boldsymbol{\mu}_{22}$ as the two particles are identical. The steady-state solution of Eqn. (4) in frequency space is derived easily by a Fourier transformation as

$$\mathbf{R}(\omega) = (-i\omega\boldsymbol{\delta} + \mathbf{A})^{-1}\mathbf{M}\boldsymbol{\xi}(\omega) \tag{5}$$

where $\mathbf{A} = \begin{bmatrix}\mu k_1\boldsymbol{\delta} & \boldsymbol{\mu}_{12}k_2\\ \boldsymbol{\mu}_{21}k_1 & \mu k_2\boldsymbol{\delta}\end{bmatrix}$ and $\mathbf{M} = \begin{bmatrix}\mu\boldsymbol{\delta} & \boldsymbol{\mu}_{12}\\ \boldsymbol{\mu}_{21} & \mu\boldsymbol{\delta}\end{bmatrix}$. $\boldsymbol{\delta}$ is 3×3 unit matrix.

1. Correlation functions

The correlation matrix can be written as

$$\langle \mathbf{R}(\omega)\mathbf{R}^\dagger(\omega)\rangle = (-i\omega\boldsymbol{\delta} + \mathbf{A})^{-1}\mathbf{M}\langle\boldsymbol{\xi}(\omega)\boldsymbol{\xi}^\dagger(\omega)\rangle\mathbf{M}(i\omega\boldsymbol{\delta} + \mathbf{A}^T)^{-1}$$

$$\frac{1}{2k_BT}\boldsymbol{C}_{\Delta\Delta} = (-i\omega\boldsymbol{\delta} + \mathbf{A})^{-1}\mathbf{M}(i\omega\boldsymbol{\delta} + \mathbf{A}^T)^{-1} \tag{6}$$

since, $\mathbf{M}\langle\boldsymbol{\xi}(\omega)\boldsymbol{\xi}^\dagger(\omega)\rangle\mathbf{M} = 2k_BT \times \mathbf{M}$. We represent the correlation function by $\boldsymbol{C}_{\Delta\Delta}$, i.e., $\langle\mathbf{R}(\omega)\mathbf{R}^\dagger(\omega)\rangle = \boldsymbol{C}_{\Delta\Delta}$. Now, for a given experimental set-up, the particles' motion can be decomposed into components parallel and perpendicular to the trap-separation. This $\boldsymbol{C}_{\Delta\Delta}$ can be decomposed into $\boldsymbol{C}_{\Delta\Delta}^{\parallel}$ and $\boldsymbol{C}_{\Delta\Delta}^{\perp}$, which correspond to motion along the trap separation and perpendicular to it, respectively. Here, we are interested only in the parallel component since, from the expressions of the parallel and perpendicular components of μ_{ij} ($\mu_{ij}^{xx} = \frac{1}{8\pi\eta a_i} = \left(2 - \frac{4a_i^2}{3r_0^2}\right)$ and $\mu_{ij}^{yy} = \frac{1}{8\pi\eta a_i} = \left(1 + \frac{2a_i^2}{3r_0^2}\right)$, with a_i being the particle radius and r_0 the inter-particle separation, it is clear that they differ only quantitatively - and moreover, the perpendicular component is lower in magnitude by a factor of two compared to the parallel component at large inter-particle separations ($r_0 >> a$). Considering remote boundaries, the translational symmetry of the friction tensor can be used to express it in the following manner:

$$\boldsymbol{\gamma}_{ij} = \gamma_{ij}^{\parallel}(\boldsymbol{r}_0)\hat{\boldsymbol{r}}_0\hat{\boldsymbol{r}}_0 + \gamma_{ij}^{\perp}(\boldsymbol{r}_0)(\boldsymbol{I} - \hat{\boldsymbol{r}}_0\hat{\boldsymbol{r}}_0)$$

Here, $\boldsymbol{r}_0$ is the trap-center separation, $\gamma_{ij}^{\parallel}(\boldsymbol{r}_0)$ is the friction coefficient for the motion parallel to $\boldsymbol{r}_0$ and $\gamma_{ij}^{\perp}(\boldsymbol{r}_0)$ is the same but for the motion perpendicular to the trap-center separation. Corresponding mobility matrices are given by $\gamma_{ik}^{\parallel}\mu_{kj}^{\parallel} = \delta_{ij}$. Now,

$$\boldsymbol{C}^{\|}_{\Delta\Delta} = (-i\omega\boldsymbol{\delta} + \mathbf{A})^{-1}_{\|}\mathbf{M}_{\|}(i\omega\boldsymbol{\delta} + \mathbf{A}^{T}_{\|})^{-1} = \frac{1}{(DetA_{\|} - \omega^2)^2 + \omega^2(TrA_{\|})^2}$$
$$\times \begin{bmatrix} \mu^{\|}k_2 - i\omega & -\mu^{\|}_{12}k_2 \\ -\mu^{\|}_{21}k_1 & \mu^{\|}k_1 - i\omega \end{bmatrix} \begin{bmatrix} \mu^{\|} & \mu^{\|}_{12} \\ \mu^{\|}_{21} & \mu^{\|} \end{bmatrix} \begin{bmatrix} \mu^{\|}k_2 + i\omega & -\mu^{\|}_{12}k_2 \\ -\mu^{\|}_{21}k_1 & \mu^{\|}k_1 + i\omega \end{bmatrix}$$
$$= \frac{1}{(DetA_{\|} - \omega^2)^2 + \omega^2(TrA_{\|})^2} \times \begin{bmatrix} \mu^{\|}k_2^2 DetM_{\|} + \mu^{\|}\omega^2 & -(DetA_{\|} - \omega^2)\mu^{\|}_{21} \\ -(DetA_{\|} - \omega^2)\mu^{\|}_{12} & \mu^{\|}k_1^2 DetM_{\|} + \mu^{\|}\omega^2 \end{bmatrix}$$

So,

$$\begin{bmatrix} C^{\|}_{11} & C^{\|}_{12} \\ C^{\|}_{21} & C^{\|}_{22} \end{bmatrix} = \frac{2K_BT}{(DetA_{\|} - \omega^2)^2 + \omega^2(TrA_{\|})^2} \begin{bmatrix} \mu^{\|}k_2^2 DetM_{\|} + \mu^{\|}\omega^2 & -(DetA_{\|} - \omega^2)\mu^{\|}_{21} \\ -(DetA_{\|} - \omega^2)\mu^{\|}_{12} & \mu^{\|}k_1^2 DetM_{\|} + \mu^{\|}\omega^2 \end{bmatrix}$$

The auto-correlations of the Brownian position fluctuations of the particles in the traps of stiffnesses k_1 and k_2 in the frequency domain are given by

$$C^{\|}_{11}(\omega) = \frac{2K_BT(\mu^{\|}k_2^2 DetM_{\|} + \mu^{\|}\omega^2)}{(DetA_{\|} - \omega^2)^2 + \omega^2(TrA_{\|})^2} \tag{7}$$

$$C^{\|}_{22}(\omega) = \frac{2K_BT(\mu^{\|}k_1^2 DetM_{\|} + \mu^{\|}\omega^2)}{(DetA_{\|} - \omega^2)^2 + \omega^2(TrA_{\|})^2} \tag{8}$$

respectively and

$$C^{\|}_{12}(\omega) = C^{\|}_{21}(\omega) = \frac{2K_BT\mu^{\|}_{21}(\omega^2 - DetA_{\|})}{(DetA_{\|} - \omega^2)^2 + \omega^2(TrA_{\|})^2} \tag{9}$$

is the representation of the cross-correlation function in frequency domain.

$$\begin{aligned} DetA_{\|} &= k_1k_2(\mu^{\|}_{11}\mu^{\|}_{22} - \mu^{\|}_{12}\mu^{\|}_{21}) \\ TrA_{\|} &= k_1\mu^{\|}_{11} + k_2\mu^{\|}_{22} \end{aligned} \tag{10}$$

Now, Eqns (7), (8) and (9) can be inverse Fourier transformed to get auto and cross-correlations in the time domain. The auto-correlations are given by

$$C^{\|}_{11}(\tau) = \frac{2K_BT}{\chi(k_1+k_2)^3}\times \left[\frac{\left(k_2^2\left(1 - \frac{\mu^{\|2}_{12}}{\mu^{\|2}_{11}}\right) - \frac{(k_1+k_2)^2(1-\chi)^2}{4}\right)\exp\left(-\beta_-\tau\right)}{1-\chi} + \frac{\left(\frac{(k_1+k_2)^2(1+\chi)^2}{4} - k_2^2\left(1 - \frac{\mu^{\|2}_{12}}{\mu^{\|2}_{11}}\right)\right)\exp\left(-\beta_+\tau\right)}{1+\chi}\right] \tag{11}$$

$$C^{\|}_{22}(\tau) = \frac{2K_BT}{\chi(k_1+k_2)^3}\times \left[\frac{\left(k_1^2\left(1 - \frac{\mu^{\|2}_{12}}{\mu^{\|2}_{11}}\right) - \frac{(k_1+k_2)^2(1-\chi)^2}{4}\right)\exp\left(-\beta_-\tau\right)}{1-\chi} + \frac{\left(\frac{(k_1+k_2)^2(1+\chi)^2}{4} - k_1^2\left(1 - \frac{\mu^{\|2}_{12}}{\mu^{\|2}_{11}}\right)\right)\exp\left(-\beta_+\tau\right)}{1+\chi}\right] \tag{12}$$

and the cross-correlation is

$$C^{\|}_{12}(\tau) = C^{\|}_{21}(\tau) = \frac{K_BT\mu^{\|}_{12}}{\sqrt{\gamma^2 - 4\omega_0^2}}\left[\exp\left(-\beta_+\tau\right) - \exp\left(-\beta_-\tau\right)\right] \tag{13}$$

where

$$\chi = \sqrt{\left[1 - \frac{4k_1k_2\left(1 - \frac{\mu^{\|2}_{12}}{\mu^{\|2}_{11}}\right)}{(k_1+k_2)^2}\right]}$$

$$\beta_- = \frac{\mu^{\|}_{11}\left(k_1+k_2\right)\left(1-\chi\right)}{2}$$

$$\beta_+ = \frac{\mu^{\|}_{11}\left(k_1+k_2\right)\left(1+\chi\right)}{2}$$

and $\gamma = TrA_{\|}$, $\omega_0^2 = DetA_{\|}$. Here we assumed $\mu^{\|}_{11} = \mu^{\|}_{22}$ and $\mu^{\|}_{12} = \mu^{\|}_{21}$, since the particles are identical. $\mu^{\|}_{ii} = \frac{1}{6\pi\eta a_i}$ and $\mu^{\|}_{ij} = \frac{1}{8\pi\eta a_i}\left(2 - \frac{4a_i^2}{3r_0^2}\right)$.

2. Complex shear modulus

Now, if we consider one of the two particles as probe to investigate the viscous and elastic nature of the system, then this will be manifested by the mean-square displacement (MSD) of it's Brownian fluctuation through the equation given below [3].

$$G^*(\omega) = \frac{k_i}{6\pi a_i}\left[\frac{2\left\langle R_i^2\right\rangle}{i\omega\left\langle \Delta\hat{R}_i^2(\omega)\right\rangle} - 1\right] \tag{14}$$

$G^*(\omega)$ is the frequency dependent dynamic complex modulus, the real part (elastic modulus) of which represents the amount of energy stored and the imaginary part (viscous modulus) represents dissipation of energy. k_i is the stiffness of the i-th trap in which the probe is confined, a_i is the radius of the probe. $\left\langle \Delta\hat{R}_i^2(\omega)\right\rangle$ is the Fourier transform of the time dependent MSD of the thermal position fluctuation of the probe particle. $\left\langle R_i^2\right\rangle$ is the time independent variance.

Single trapped particle in a viscous fluid: For a single trapped particle in a viscous medium, the position autocorrelation is given by

$$\langle R(\tau)R(0)\rangle = \frac{K_B T}{k}\exp(-\omega_c\tau) \tag{15}$$

where, $\omega_c = \frac{k}{6\pi\eta a_0}$ and k is the corresponding trap stiffness. Therefore, the time-dependent mean-square displacement (MSD) is

$$\begin{aligned}\left\langle \Delta R^2(\tau)\right\rangle &= 2\left[\left\langle R^2(0)\right\rangle - \langle R(\tau)R(0)\rangle\right] \qquad (16)\\ &= \frac{2K_BT}{k}\left[1-\exp\left(-\omega_c\tau\right)\right] \qquad (17)\end{aligned}$$

Now, from the Eqn. (14), in the following manner we can calculate the complex shear modulus $G^*(\omega)$ of the surrounding fluid accessed by the single trapped particle.

$$\begin{aligned}G^*(\omega) &= G(s)|_{s=i\omega}\\ &= \frac{k}{6\pi a_0}\left[\frac{2\left\langle R^2\right\rangle}{s\left\langle \Delta\hat{R}^2(s)\right\rangle} - 1\right]\Bigg|_{s=i\omega}\\ &= i\eta\omega\end{aligned}$$

Here, a_0 is the particle radius, $\left\langle \Delta\hat{R}^2(s)\right\rangle$ is the Laplace transformation of the MSD and s is the Laplace frequency. Clearly thus, the surrounding medium accessed by the single trapped particle is purely dissipative in nature.

Two particles trapped near to each other in a viscous fluid: Now, for a system of two trapped particles close to each other we can go through similar process assuming one of the pair of trapped particles as probe. From Eqns. (11) and (12), we can, in general write the autocorrelation function (ACF) for the probe in the i-th position as

$$C_{ii}^{\|}(\tau) = \frac{2K_BT}{\chi(k_i+k_j)^3}\times \left[\frac{\left(k_j^2\left(1-\frac{\mu_{ij}^{\|2}}{\mu_{ii}^{\|2}}\right) - \frac{(k_i+k_j)^2(1-\chi)^2}{4}\right)\exp\left(-\beta_-\tau\right)}{1-\chi} + \frac{\left(\frac{(k_i+k_j)^2(1+\chi)^2}{4} - k_j^2\left(1-\frac{\mu_{ij}^{\|2}}{\mu_{ii}^{\|2}}\right)\right)\exp\left(-\beta_+\tau\right)}{1+\chi}\right]$$

where, i, $j = 1$, 2 and $i \neq j$. The stiffness of the i-th trap is k_i. Further, we can write the ACF as

$$C_{ii}^{\|}(\tau) = A\exp\left(-\beta_-\tau\right) + B\exp\left(-\beta_+\tau\right)$$

where,

$$A = \frac{2K_BT}{\chi(k_i+k_j)^3}\left[\frac{k_j^2\left(1-\frac{\mu_{ij}^{\|2}}{\mu_{ii}^{\|2}}\right) - \frac{(k_i+k_j)^2(1-\chi)^2}{4}}{1-\chi}\right]$$

and

$$B = \frac{2K_BT}{\chi(k_i+k_j)^3}\left[\frac{\frac{(k_i+k_j)^2(1+\chi)^2}{4} - k_j^2\left(1-\frac{\mu_{ij}^{\|2}}{\mu_{ii}^{\|2}}\right)}{1+\chi}\right]$$

Therefore, the corresponding MSD is given by

$$\left\langle \Delta R_i^2(\tau)\right\rangle = 2\left[(A+B) - A\exp\left(-\beta_-\tau\right) - B\exp\left(-\beta_+\tau\right)\right]$$

Now, if we consider the particle of radius a_i in the i-th trap as probe, then the complex shear modulus is given by

$$\begin{aligned}G^*(\omega) &= G(s)|_{s=i\omega}\\ &= \frac{k_i}{6\pi a_i}\left[\frac{2\left\langle R_i^2\right\rangle}{s\left\langle \Delta\hat{R}_i^2(s)\right\rangle} - 1\right]\Bigg|_{s=i\omega}\end{aligned}$$

where, $\left\langle \Delta\hat{R}_i^2(s)\right\rangle$ is the Laplace transformation of the MSD of the probe and $\left\langle R_i^2\right\rangle$ is the variance of the corresponding thermal fluctuations. This results into,

$$G^*(\omega) = \frac{k_i}{6\pi a_i}\Bigg[\omega^2\Bigg\{\frac{(A\beta_- + B\beta_+)(A\beta_+ + B\beta_-)}{\omega^2(A\beta_- + B\beta_+)^2 + \beta_+^2\beta_-^2(A+B)^2} - \frac{\beta_+\beta_-(A+B)^2}{\omega^2(A\beta_- + B\beta_+)^2 + \beta_+^2\beta_-^2(A+B)^2}\Bigg\} + i\omega\Bigg\{\frac{(A+B)(A\beta_+ + B\beta_-)\beta_+\beta_-}{\omega^2(A\beta_- + B\beta_+)^2 + \beta_+^2\beta_-^2(A+B)^2} + \frac{\omega^2(A+B)(A\beta_- + B\beta_+)}{\omega^2(A\beta_- + B\beta_+)^2 + \beta_+^2\beta_-^2(A+B)^2}\Bigg\}\Bigg] \tag{18}$$

However, this expression can be simplified substantially. The real part of the $G^*(\omega)$ can be simplified to

$$G'(\omega) = \frac{k_i}{6\pi a_0} \times \omega^2 \left[\frac{AB(\beta_+ - \beta_-)^2}{\omega^2(A\beta_- + B\beta_+)^2 + \beta_+^2\beta_-^2(A+B)^2}\right] \tag{19}$$

Further, it can be shown that

$$\left.\begin{aligned} A + B &= \left(\frac{K_B T}{k_i}\right) \\ AB &= \frac{(K_B T)^2}{\gamma^2 - 4\omega_0^2} \times \frac{k_j \mu_{ij}^2}{k_i} \\ \beta_+ + \beta_- &= \gamma \\ \beta_+ - \beta_- &= \sqrt{\gamma^2 - 4\omega_0^2} \\ \beta_+\beta_- &= \omega_0^2 \\ A\beta_- + B\beta_+ &= \mu_{ii} K_B T \\ A\beta_+ + B\beta_- &= \mu_{ii} K_B T \frac{k_j}{k_i} \end{aligned}\right\} \tag{20}$$

From this expressions above (20), one can get simplified forms of A, B, β_+ and β_-.

$$\left.\begin{aligned} A &= \frac{K_B T}{2k_i}\left[1 + (k_j - k_i)\sqrt{\frac{1}{(k_j - k_i)^2 + \frac{4k_i k_j \mu_{ij}^{\parallel 2}}{\mu_{ii}^{\parallel 2}}}}\right] \\ B &= \frac{K_B T}{2k_i}\left[1 - (k_j - k_i)\sqrt{\frac{1}{(k_j - k_i)^2 + \frac{4k_i k_j \mu_{ij}^{\parallel 2}}{\mu_{ii}^{\parallel 2}}}}\right] \end{aligned}\right\} \tag{21}$$

$$\left.\begin{aligned} \beta_- &= \frac{\mu_{ii}^{\parallel}\left[(k_i + k_j) - \sqrt{(k_j - k_i)^2 + \frac{4k_i k_j \mu_{ij}^{\parallel 2}}{\mu_{ii}^{\parallel 2}}}\right]}{2} \\ \beta_+ &= \frac{\mu_{ii}^{\parallel}\left[(k_i + k_j) + \sqrt{(k_j - k_i)^2 + \frac{4k_i k_j \mu_{ij}^{\parallel 2}}{\mu_{ii}^{\parallel 2}}}\right]}{2} \end{aligned}\right\} \tag{22}$$

Substituting the above expressions (20) in the Eqn. (19), we finally get,

$$G'(\omega) = \frac{k_i}{6\pi a_i} \times \omega^2 \left[\frac{k_i k_j \mu_{ij}^2}{\omega_0^4 + (\mu_{ii} k_i)^2 \omega^2}\right] \tag{23}$$

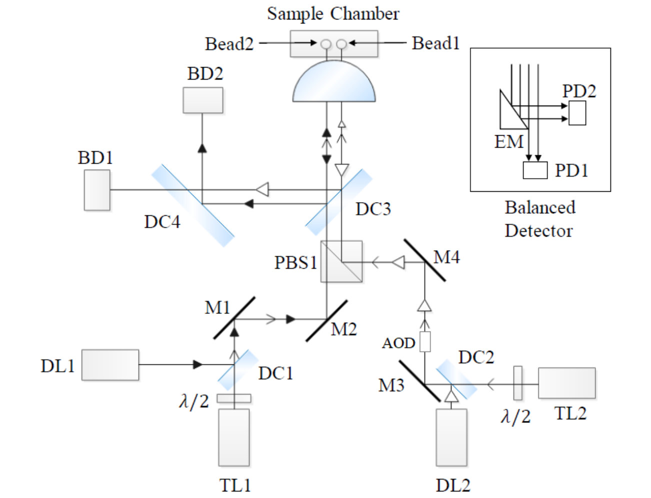

Figure 1: Schematic of the experimental setup. $\lambda/2$: half-wave plate, AOD: Acousto-optic deflector, M: plane mirror, DC: dichroic, TL: trapping laser, DL: detection laser, PBS: polarizing beam splitter, BD: balance detector, EM: edge mirror, PD: photo-diode (Thorlabs PDA100A-EC).

Similarly, we get the imaginary part of $G^*(\omega)$ as

$$G''(\omega) = \frac{k_i}{6\pi a_i} \times \omega \left[\frac{k_j \mu_{ii}\omega_0^2 + k_i \mu_{ii}\omega^2}{\omega_0^4 + (\mu_{ii} k_i)^2 \omega^2}\right] \tag{24}$$

II. EXPERIMENT

To check the validity of the above-described theory we set up (Fig. 1) a dual-beam optical tweezers by focusing two independently generated orthogonally polarized laser beams from two diode lasers (TL1 and TL2) of wavelength $\lambda = 1064$ nm, using a high NA immersion-oil microscope objective (Zeiss PlanApo,100 × 1.4). Two $\lambda/2$ plates, in front of the lasers control the polarization angle of these two laser beams. After passing through $\lambda/2$ plates one of these two beams encounter an acousto-optic deflector (AOD) to modulate the direction of the beam and then mirror pairs M1, M2 and M3, M4, respectively, as two beam steerers. Then they get coupled into a polarizing beam splitter (PBS1). For detection, we use two lasers of wavelength $\lambda = 671$ nm (DL1) and $\lambda = 780$ nm (DL2) which we couple to the trapping lasers using two dichroic mirrors (DC1 and DC2) before the beam steering mirrors. We image two trapped beads and measure their displacements by back-focal-plane-interferometry, while we use white light for imaging. After collecting the total back-scattered light from the microscope, we separate the components from the two particles using another dichroic (DC4) and then direct these towards two balanced detection systems BD1 and BD2, developed using photodiode pairs. The cartoon representation of one such balanced detector is shown in the inset of Fig. 1. The voltage-amplitude calibration of our detection system reveals that we can resolve motion of around 5 nm with an SNR of 2. We prepared a very low volume fraction sample ($\phi \approx 0.01$) with 3 μm diameter polystyrene latex beads in 1 M NaCl-water solution for avoiding surface charges. We loaded the sample in a chamber of area 20×10 mm and height 0.2 mm and two spherical polystyrene beads (Sigma LB-30) of mean size 3 μm each were trapped in two calibrated optical traps which we kept separated initially by a distance of 5 ± 0.1 micron from each other, and at a distance of 30 μm from the nearest wall. Then the separation and laser powers were varied to perform our experiment. According to a reported experimental work [4], this distance is large enough to avoid optical cross-talk and the effects from surface charges. In order to ensure that the trapping beams do not influence each other, we measured the Brownian motion of one when the other is switched on (in the absence of a particle), and checked that there were no changes in the properties of the Brownian fluctuations. We normalized each time series representing the position fluctuation of each particle by the sum intensity measured by the corresponding photodiode pair to account for the laser power fluctuations. Then we collected it, typically over 10 second and at sampling frequency 10kHz using a data acquisition card (NI USB-6356), which was coupled to a computer. we recorded two time series corresponding to two trapped particles simultaneously. We check that there is less than one percent cross-talk of signals in the two detectors due to leakage through the dichroic DC4. Further, to avoid low frequency noise for the measurement of G^*, we perform active microrheology by modulating one of the trapped particles by the AOD in the presence of the other, and measure the response of the corresponding confined particle over 5 minutes for each frequency of modulation.

III. CALIBRATION AND ANALYSIS

Calibration: Before performing the experiments, it is essential to calibrate the traps properly. First and foremost, we need to ensure that both the traps are independent of each other, i.e., there is no optical cross-talk present between the traps. Understandably, any cross-talk between the traps will distort the harmonic nature of the potentials as a consequence of which the position probability distribution function will deviate from being Gaussian. To ensure the absence of any optical cross-talk, we confine a particle in an individual trap keeping the adjacent trap empty (however, the corresponding trapping laser is still on) and record its thermal position fluctuations in order to measure the corresponding probability distribution function. We perform this check for all the separations, and in Fig. 2, we show the results for the closest and for the farthest distances that we use in our experiment. It is clear from this figure that the optical cross-talk between the traps is absent for the whole range of the trap separations used in our experiment, as none of the position probability distribution functions deviate from their expected Gaussian nature. Note that, according to the work reported in the Ref. [4], 5 μm separation between two particles of radius 1.5 μm is large enough to prevent any cross-talk. Careful sensitivity measurement of the detection system is required for our experiments, which we perform by sifting the trapping beam by a known amount and detecting the corresponding change in the signal from the balanced detection system.

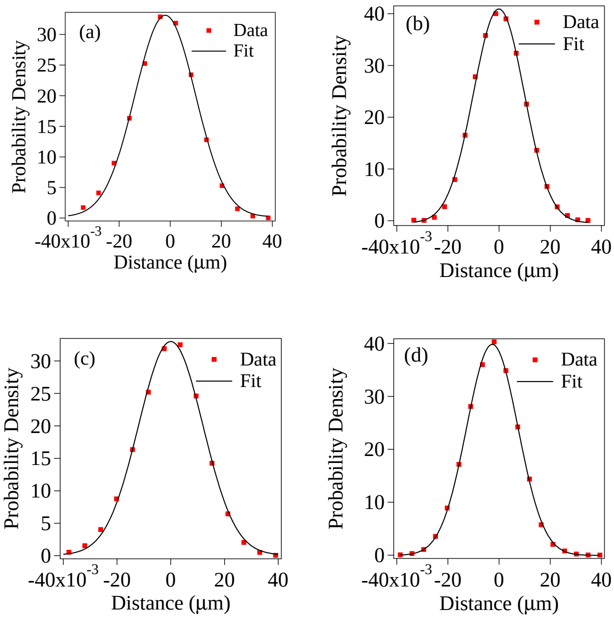

Figure 2: Position probability density functions of the trapped particles for trap separations (a-b) 5 μm and (c-d) 9 μm. (a), (c) are for the weak traps of stiffness $k_2 = 30$ μN/m and (b), (d) are for the strong traps of stiffness $k_1 = 43$ μN/m.

Now, to measure the stiffnesses of the traps we use the power spectral density (PSD) method which in addition can calculate the diffusion coefficient and thus can cross-check the measured sensitivity values. However, we cross-check the measured stiffnesses from the PSD with the measurement using the equipartition theorem and get very close match (maximum within 0.5 %; the small discrepancy, we perceive, is due to the fitting error in the PSD method or due to a small additive noise in the data that does not get reflected in f_c but affects the variance, which governs the equipartition theorem). The equipartition theorem ($\langle\langle(x^2)\rangle = \frac{K_B T}{k}$; the mean has been assumed

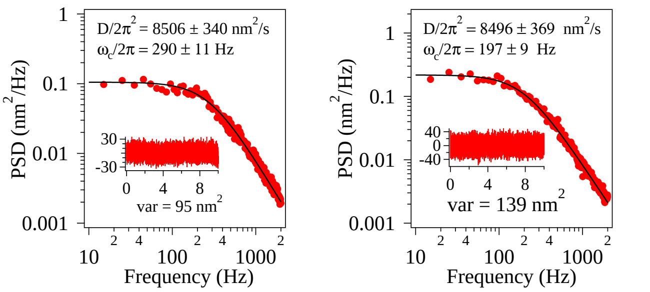

Figure 3: Data representing the stiffness measurement process along with the fitted parameter values. (Left) The measured PSD (red circles) and the corresponding fit (black solid line) w.r.t. frequency, representing the highest stiffness of a mean value 43 ± 0.7 μN/m (over several data sets); in the inset raw data of 10 seconds has been shown in *nm* units. (Right) The similar measurement representing stiffness of a mean value 30 ± 0.6 μN/m (over several data sets).

to be zero) is independent of the rheological properties of the surrounding environment which thus remains less affected even by the presence of any other particles around it. The power spectral density function of a particle confined in an optical trap (harmonic potential) is given by

$$S_{xx}(f) = \frac{D/2\pi^2}{f^2 + f_c^2} \tag{25}$$

where, $f_c = \frac{k}{12\pi^2 \eta a_0}$, k is the trap stiffness, η is the viscosity of the surrounding fluid and a_0 is the radius of the particle. To measure the stiffness from the PSD, we follow the procedure suggested in Ref. [5–7], and block data with a bin size of 100 points and fit with the desired theoretical expression as given in the Eqn. (25). Also, we set the frequency range for fitting over a range in order to avoid the systematic low and high frequency errors caused due to very low frequency noises and the aliasing effect respectively. We show two set of data representing our whole stiffness measurement process in Fig. 3, where it also can be seen that the estimated value of the diffusion coefficient from the PSD matches the corresponding value for water at temperature 300 K. For each configuration, we perform the stiffness measurement over several sets of data and observe a standard deviation of maximum 4%. In increasing the trap separation, the stiffness changes, which we however bring back to the desired value by tuning the laser power.

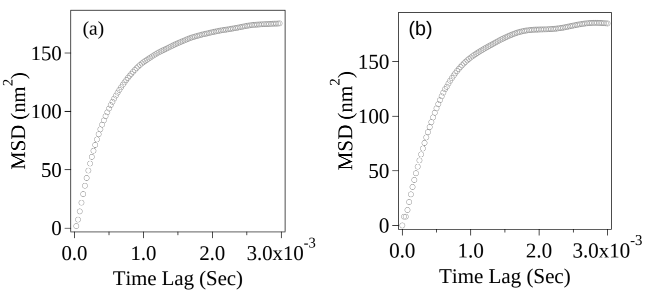

Figure 4: MSD of the position fluctuation of the probe confined in trap of stiffness $k_1 = 43$ μN/m when the other trap with an identical particle in it has stiffness (a) $k_2 = 36.5$ μN/m, (b) $k_2 = 10$ μN/m.

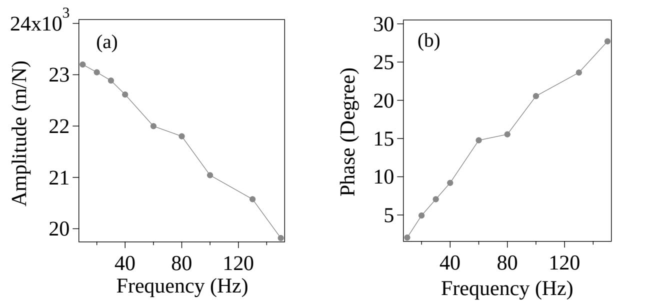

Figure 5: (a) Amplitude and (b) phase of the probe confined in trap of stiffness $k_1 = 43$ μN/m when the other trap with an identical particle in it has stiffness $k_2 = 10$ μN/m.

Analysis: In order to study the induced memory in the system, we calculate the auto-correlation function (ACF) and the corss-correlation function (CCF) of the thermal position fluctuations of the trapped particles in the two traps of various stiffnesses and at different separations. Further, we use one of the trapped particles as probe and use Eqn. (14) to measure the complex shear modulus $G^*(\omega)$ of the surrounding environment. Note that in Eqn. (14), we subtract the contribution of the trap to G^*, which is $\frac{k_i}{6\pi a_i}$. We perform passive microrheology for the higher side of the frequency spectrum to avoid various low frequency noises, and for the lower part of the spectrum we use active microrheology to calculate G^*, as active microrheology has better signal-to-noise ratio w.r.t. the passive microrheology. For passive microrheology we use Eqn. (14) which uses the MSD of the probe particle. Now for doing the measurement from the MSD, we need to take the Fourier transform of the measured MSD of the probe. However, we do not directly calculate the Fourier transform to avoid the potential errors that can be caused by the process principally at the extreme frequency ends. These arise while working with a limited number of points for a finite time. In contrast to the direct Fourier transform of the MSD, we follow the power law expansion method described by T. G. Mason in Ref. [8]. In Fig. 4, we have shown MSDs of the probe for two stiffness values of the nearby trap which confines an identical particle in it. In addition, to demonstrate that the extraction of G^* from the MSD is independent of the trap stiffness, we have plotted G^* for a single trap for different stiffnesses in the same graph (Fig. 6). However, since, the real and the imaginary parts of G^* do not depend on the stiffness of the trap, they almost overlap on each other.

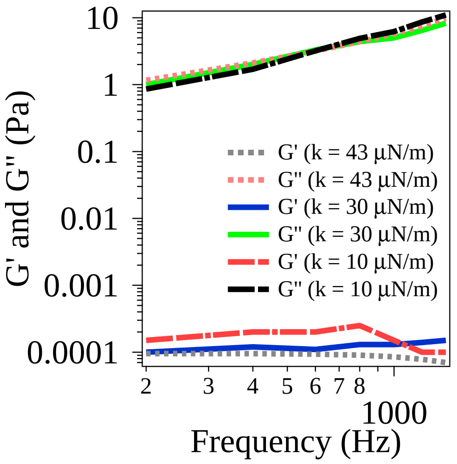

Figure 6: Real and imaginary parts of G^* w.r.t frequency for single trap of various trap stiffnesses.

For the active microrheology, we can solve the generalized Langevin equation describing the motion of a particle in a viscoelastic fluid with an additional forcing term included and neglecting the noise and the inertial term from it. Note that we are only interested about the response of the particle under external perturbation, and we work in a frequency regime where the inertial effect is negligible. The corresponding equation in the frequency domain is given by,

$$0 = i\omega\gamma(\omega) - kx(\omega) + kx_0(\omega) \tag{26}$$

where $x(\omega)$ is the position of the particle, $\gamma(\omega)$ is the frequency dependent damping term, k is the stiffness of the trap and $x_0(\omega)$ is the external perturbation. Therefore, the particle response function is given by

$$\chi_{res}(\omega) = \frac{1}{k - i\omega\gamma(\omega)} \tag{27}$$

where the response function is defined as,

$$x(\omega) = \chi_{res}(\omega)kx_0(\omega) \tag{28}$$

Now, the complex shear modulus $G^*(\omega)$ is related to $\gamma(\omega)$ as $G^*(\omega) = -i\omega\gamma(\omega)/6\pi a_i$; a_i is the radius of the probe particle [9]. So,

$$G^*(\omega) = \frac{1}{6\pi a_i \chi_{res}(\omega)} - \frac{k}{6\pi a_i} \tag{29}$$

and $G^*(\omega) = G'(\omega) - iG''(\omega)$. Note that here also we subtract the contribution of the trap to $G^*(\omega)$. In the experiment, we modulate the trap of stiffness 43μN/m with an amplitude of 100 nm using the AOD and measure the response of the particle for each frequency over 5 min. Further, we use Eqn. (28) to calculate the corresponding response function from the data, and use Eqn. (29) to calculate the $G^*(\omega)$ value. In Fig. 5, we have shown one of our measurements of the amplitude and phase of the response function for the probe trap stiffness at 43μN/m and the other trap stiffness at 10μN/m. Note that we have performed similar experiments earlier and this method has been validated by us rigorously [10, 11].

[1] C. Gardiner, *Phys. Rev. A*, 1984, **29**, 2814.
[2] C. Gardiner, *Handbook of stochastic methods. vol. 4 Springer*, 1985.
[3] M. Tassieri, G. M. Gibson, R. Evans, A. M. Yao, R. Warren, M. J. Padgett and J. M. Cooper, *Phys. Rev. E*, 2010, **81**, 026308.
[4] A. Stilgoe, N. Heckenberg, T. Nieminen and H. Rubinsztein-Dunlop, *Phys. Rev. Lett.*, 2011, **107**, 248101.
[5] K. Berg-Sørensen and H. Flyvbjerg, *Review of Scientific Instruments*, 2004, **75**, 594–612.
[6] S. F. Tolić-Nørrelykke, E. Schäffer, J. Howard, F. S. Pavone, F. Jülicher and H. Flyvbjerg, *Review of scientific instruments*, 2006, **77**, 103101.
[7] S. F. Nørrelykke and H. Flyvbjerg, *Review of Scientific Instruments*, 2010, **81**, 075103.
[8] T. G. Mason, *Rheologica Acta*, 2000, **39**, 371–378.
[9] M. Grimm, S. Jeney and T. Franosch, *Soft Matter*, 2011, **7**, 2076–2084.
[10] S. Paul, A. Laskar, R. Singh, B. Roy, R. Adhikari and A. Banerjee, *Phys. Rev. E*, 2017, **96**, 050102(R).
[11] S. Paul, R. Kumar and A. Banerjee, *Phys. Rev. E*, 2018, **97**, 042606.